


Cite this: *RSC Adv.*, 2023, 13, 1757

# Photophysical and anion sensing properties of a triphenylamine–dioxaborinine trimeric compound†

Alexis Tigreros,<sup>a</sup> Camilo Bedoya-Malagón,<sup>b</sup> Alejandra Valencia,<sup>b</sup> Mayerlin Núñez-Portela<sup>b</sup> and Jaime Portilla<sup>a\*</sup>

Herein, we report the synthesis and photophysical characterization of the novel tris(4-(2,2-difluoro-6-methyl-2H-1λ<sup>3</sup>,3,2λ<sup>4</sup>-dioxaborinin-4-yl)phenyl)amine trimeric probe (**A2**) via the reaction between triphenylamine (**1**), acetic anhydride, and BF<sub>3</sub>·OEt<sub>2</sub> implying the twelve new bond formation in a one-pot manner. This highly fluorescent compound in solution ( $\phi$  up to 0.91 at 572 nm) and solid state ( $\phi$  = 0.24 at 571 nm) showed a better solvatochromism than its analog monomeric **A1** due to symmetry-broken charge transfer, which is consistent with high solvent dipolarity (SdP) response in Catalán's multiparametric regression. Notably, **A2** had a high sensibility and selectivity for CN<sup>−</sup> or F<sup>−</sup> in solution (LODCN<sup>−</sup>/F<sup>−</sup> = 0.18/0.70 μM), and CN<sup>−</sup> can be discriminated from F<sup>−</sup> by the reaction of **A2** with 3.0 equiv. of CN<sup>−</sup>. In addition, **A2** was impregnated on filter paper to prepare test strips that were applied to naked-eye qualitative sensing of CN<sup>−</sup> or F<sup>−</sup>. Finally, the octupolar system in **A2** allows for better action of two-photon excitation cross-section values when compared with that of the dipolar structure in **A1**. These findings provide further information for the design of new efficient two-photon absorption dyes.

Received 25th November 2022  
Accepted 29th December 2022

DOI: 10.1039/d2ra07498b

rsc.li/rsc-advances

## Introduction

Boron complex-containing molecules are an interesting and extensively used class of organic fluorescent compounds. These dyes have valuable photophysical properties such as strong absorption bands, high fluorescent quantum yields ( $\phi$ ), good solubility in organic solvents, photostability, microenvironment-dependent emission, *etc.*<sup>1–3</sup> Therefore, this important family of organic fluorophores can serve in numerous applications involving bioimaging probes,<sup>4</sup> photosensitizers in photodynamic therapy,<sup>5</sup> red-emitting complexes with a mega-large Stokes shift,<sup>6</sup> multicolor fluorescent initiators,<sup>7</sup> colored triboluminescence compounds,<sup>8</sup> and fluorescent probes for mercury detection in living cells,<sup>7</sup> among others.

Importantly, some characteristic fluorophores perform through two-photon absorption (TPA) phenomena that involve the simultaneous absorption of two photons from a laser light source,<sup>9</sup> which has advantages over the classical one-photon process. For instance, a molecule can be excited with low-

energy photons *versus* the classical methods. The TPA transition probability increases with the excitation laser intensity's square giving the optical absorption's high spatial selectivity,<sup>10</sup> leading to applications in three-dimensional (3D) data storage,<sup>11</sup> photodynamic therapy,<sup>12,13</sup> 3D micro-fabrication,<sup>14</sup> and high-resolution bioimaging.<sup>15</sup> Thus, novel fluorophores development by efficient synthetic approach is highly desirable and a research-active field in chemistry, material sciences, and the industry.

Structurally, many architectures have been used to achieve good TPA responses; that is, conjugated donor (D) and acceptor (A) with different geometry organizations, dipolar (D– $\pi$ –A), quadrupolar (D– $\pi$ –A– $\pi$ –D or A– $\pi$ –D– $\pi$ –A), and octupolar (D–( $\pi$ –A)<sub>3</sub> or A–( $\pi$ –D)<sub>3</sub>),<sup>16</sup> this appreciation has been verified by theoretical and experimental results in the Jean-Luc Brédas research group.<sup>17</sup> In this way, the electronic connecting between strategic fluorophores is a good tactic for designing dyes with TPA properties; for example, hybrid fluorophores containing triphenylamine (TPAm) or the boron complex dioxaborinine (DB) have been used for this purpose.<sup>9,18</sup>

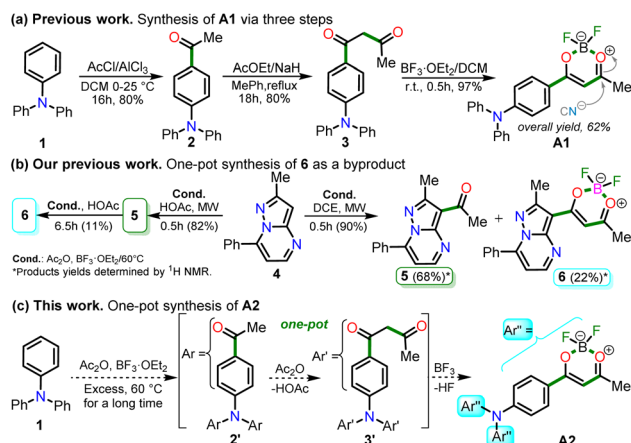
In 2020, Tamilarasan *et al.*<sup>19</sup> synthesized the dipolar dye **A1** (Scheme 1a) based on a triphenylamine–dioxaborinine hybrid compound as a colorimetric and fluorimetric probe for the reversible detection of cyanide (LOD = 0.36 μM in MeCN : H<sub>2</sub>O 98 : 2). The probe was obtained in 62% global yield by a three-step sequence starting from TPAm (**1**). This synthesis involves a sequential double acetylation reaction *via* the carbonyl compounds intermediates **2** and **3**, and the final formation of

<sup>a</sup>Bioorganic Compounds Research Group, Department of Chemistry, Universidad de Los Andes, Carrera 1 No. 18A-10, Bogotá 111711, Colombia. E-mail: jportilla@uniandes.edu.co

<sup>b</sup>Quantum Optics Laboratory, Department of Physics, Universidad de Los Andes, Carrera 1 No. 18A-10, Bogotá, Colombia

† Electronic supplementary information (ESI) available: Characterization data, experimental, spectra (NMR, HRMS, absorption, and emission), green metrics, and computational details of fluorophores. See DOI: <https://doi.org/10.1039/d2ra07498b>

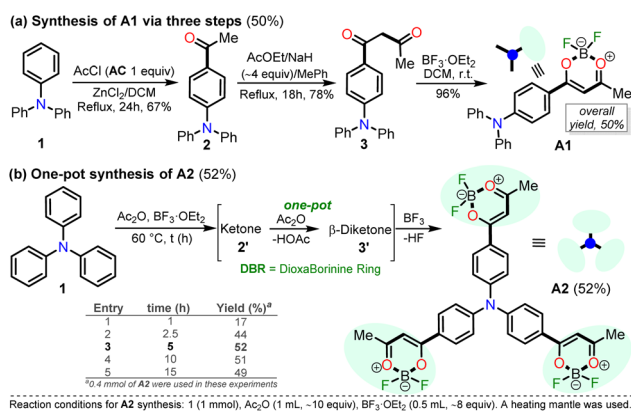




Scheme 1 Synthesis of fluorophores bearing dioxaborinine (a) **A1**,<sup>19</sup> (b) **5**, and (c) **A2**.<sup>20</sup>

the boron complex in **A1**. Recently, we carried out a  $\text{BF}_3$ -mediated synthesis of 3-acetylpyrazolo[1,5-*a*]pyrimidines (similar to **5**) under microwave (MW) irradiation and using acetic anhydride as an acetylating agent (Scheme 2b). During the optimizing reaction conditions process, we observed that the fluorescent by-product **6**, bearing the pyrazolo[1,5-*a*]pyrimidine–dioxaborinine hybrid system resulting from the formation of four new bonds in a one-pot manner, is favored in long reaction times.<sup>20</sup>

Within the most conventional photophysical applications of organic fluorophores, ion recognition has been the subject of extensive study in the last two decades;<sup>21,22</sup> in particular, cyanide ( $\text{CN}^-$ ) is one of the most concerning environmental ions. Cyanide toxicity is known because it can inhibit the mitochondrial cytochrome C oxidase and suppress oxygen transport.<sup>23,24</sup> Consequently, the development of sensitive and selective probes for the sensing of this anion has been gaining considerable attention in recent years because of its essential role in a wide variety of biological,<sup>25</sup> environmental,<sup>26</sup> biochemical,<sup>27</sup> clinical,<sup>28</sup> synthetic due to design and preparation of the respective chemosensors and industrial applications.<sup>21,22</sup>



Scheme 2 Synthesis of dioxaborinine–triphenylamine hybrid dyes (a) **A1** and (b) **A2**.

Considering the above background and our continuing interest in obtaining new functional fluorophores,<sup>20,29–31</sup> we planned to develop the octupolar dye **A2** by a synthesis implying the twelve new bonds formation in a one-pot manner (Scheme 2c). Fluorophore **A2** is a tris-dioxaborinine–triphenylamine hybrid compound with promising photophysical properties in solution and solid-state, which we wish to study and compare with those for the similar dipolar system **A1**. Explicitly, **A2** is expected to have good TPA responses with improved results over other octupolar dyes synthesized even by difficult methods involving various reaction steps;<sup>32</sup> for this purpose and as a proof-of-concept, by measuring the two-photon excitation action cross section when exciting the probes **A1** and **A2** with a continuous-wave (CW) laser at 810 nm. Ultimately, similar to **A1**,<sup>19</sup> the novel dye **A2** could be applied for cyanide sensing by fluorescent changes after a chemical reaction with the anion.

## Results and discussion

### Synthesis

For this research, the dioxaborinine–triphenylamine hybrid dyes **A1** and **A2** were synthesized. The synthetic approaches for preparing these dyes starting from triphenylamine (**1**, TPAM), are simple and proceed in good yields (Scheme 2). According to the literature,<sup>19,33,34</sup> compound **A1** was synthesized in 50% global yield *via* a three-step sequence starting from triphenylamine (**1**). Nevertheless, for **A2** synthesis, a new approach was used to convert substrate **1** into the trisubstituted derivate *via* the twelve new bonds formation in a one-pot manner in good yield (52%). In this respect, the mixture of acetic anhydride (**AA**) with boron trifluoride diethyl etherate ( $\text{BF}_3 \cdot \text{OEt}_2$ ) was used as multiple acetylating agents six times to give the respective  $\beta$ -diketone intermediate **3'** and the complexing agent of the last step. Structures for the hybrid dyes **A1** and **A2** were established by NMR spectroscopy ( $^1\text{H}$ ,  $^{13}\text{C}$ , and  $^{19}\text{F}$ ) and HRMS analysis (Fig. S1–S9†).

Remarkably, although the hybrid compounds **A1** (50%) and **A2** (52%) were obtained with close yields starting from triphenylamine (**1**), the octupolar dye **A2** requires only one step for its formation in 5 hours at 60 °C and with the twelve new bonds formation. In contrast, the dipolar derivative **A1** synthesis (Scheme 2a) consumptions three steps (*i.e.*, ring acetylation/one new bond, ketone  $\alpha$ -acetylation/one new bond, and complexation with  $\text{BF}_3$ /two new bond) through the intermediates (4-acetylphenyl)diphenylamine (**2**) and 1-(4-(diphenylamino)phenyl)butane-1,3-dione (**3**). Thus, the synthesis of **A2** implies a much better operational simplicity, lower consumption of solvents due to the solvents used as reaction medium and in the purification steps and a more excellent atomic economy concerning the probe **A1** as a result of the one-pot synthesis of **A2**.

It is important to note that the reaction time played a crucial role in **A2** synthesis since, after 1 hour at 60 °C, the product was obtained with only a 17% yield; however, the yield increased to 44% after 2.5 hours of reaction. The optimal conditions for this reaction turned out to be 5 hours at 60 °C because the yield increased to 52%, and no noticeable changes were observed during longer reaction times; with lower temperatures, the



reaction does not progress much, and with higher temperatures, by TLC, a complex mixture of products was observed (Scheme 2b). Consequently, our previous results on constructing the dioxaborinine ring are a reliable starting point for accessing various derivatives of this heterocyclic core.<sup>20</sup> Additionally, it was possible to establish that the optimum temperature to treat the acetylating mixture (an excess of  $\text{Ac}_2\text{O}/\text{BF}_3 \cdot \text{OEt}_2$ ) is 60 °C. Finally, we could verify our hypothesis that the formation of the DB ring in a one-pot manner is enhanced when long reaction times are used.

## Photophysical properties

**Solvatochromism.** Solvent-dependent optical properties of compounds **A1** and **A2** were evaluated by UV-vis absorption and emission measurements in a set of non-protic solvents (Fig. 1, Table 1, and eqn (1); see the Experimental section) such as toluene (PhMe), *tert*-butyl methyl ether (TBME), tetrahydrofuran (THF), ethyl acetate (EA), chloroform ( $\text{CHCl}_3$ ), *N,N*-dimethylformamide (DMF), and acetonitrile (MeCN).

For instance, in toluene, two absorption bands were observed for **A1** (295 and 427 nm) and **A2** (315 and 446 nm), the latter having a molar absorptivity at least twice that of **A1**. This feature is ascribed to the degeneracy of the S1 state of **A2** and the increased number of DB groups that alter the electronic energy levels of the triphenylamine core by  $\pi$ -conjugation.<sup>35</sup> Meanwhile, little to non-interaction at the ground state was noticed since there was no solvatochromism in **A1** and **A2**.

Moreover, emission bands of **A1** shift bathochromically from the weakly polar toluene ( $\lambda_{\text{em}} = 461$  nm) to the strongly polar acetonitrile ( $\lambda_{\text{em}} = 492$  nm); while **A2** displays an intense solvatochromism ( $\lambda_{\text{em}}/\text{MePh} = 484$  nm to  $\lambda_{\text{em}}/\text{MeCN} = 575$  nm), exhibiting a more dipolarity in the excited state, which may correspond to a symmetry broken dipolar state.<sup>36</sup> Catalán multiparametric regression analysis was performed to evaluate the polarity at the excited state of **A1** and **A2** (eqn (2), Table S1†). The solvent dipolarity (SdP) stabilized best the excited state of **A1** (slope =  $-1937.90 \text{ cm}^{-1}$ ,  $R^2 = 0.8862$ ) and **A2** (slope =  $-4607.54 \text{ cm}^{-1}$ ,  $R^2 = 0.9438$ ). In general, compound **A2** displays a more polar structure at the excited state when compared with **A1** (Fig. S12 and S13†). This result is consistent with previous studies demonstrating the solvent-induced symmetry-breaking charge transfer in an octupolar chromophore.<sup>35</sup> It is important to note that the branching increases the fluorescence quantum yield in a low to medium-polarity solvent (Table 1).

**Solid-state emission.** The fluorescence spectra in the solid-state of compounds **A1** and **A2** were registered under excitation at 300 nm at room temperature, and the results were fortunately very satisfactory (Fig. 2 and Table 1, entry 8). Emission of **A1** in the solid-state falls in the orange-red region (608 nm) and that of **A2** in the yellow-orange region (571 nm). Curiously, the solid-state emission spectrum of **A2** resembles that of **A2** dissolved in a high-polarity solvent. In contrast, the solid-state emission spectrum of the dipolar chromophore **A1** is highly red-shift from that in solution (498 nm in MeCN). Such a marked difference in solid-state emission of the dyes **A1** and **A2** can be related possibly to the different packing of the dipolar and octupolar molecules in the solid state.<sup>37</sup> Consequently, a strong intermolecular donor–acceptor interaction is expected

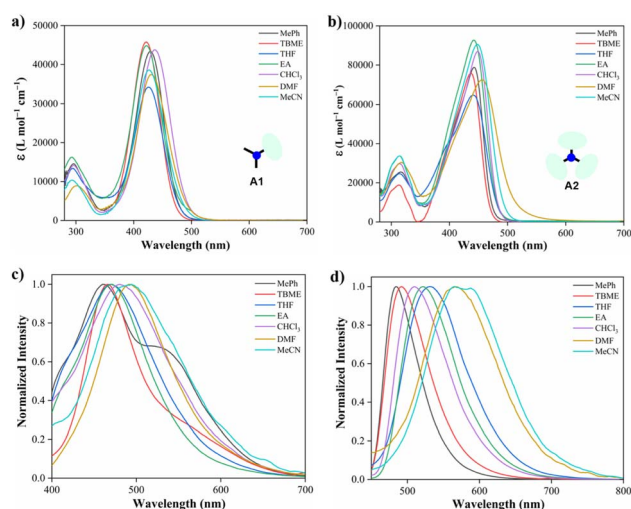


Fig. 1 Absorption and emission ( $\lambda_{\text{ex}} = 350$  nm) spectra in various solvents (10.0  $\mu\text{M}$ ) at 20 °C of hybrid compounds **A1** (a and c) and **A2** (b and d).

Table 1 Photophysical properties of the hybrid compounds **A1** and **A2**<sup>a</sup>

Entry	Solvent	<b>A1</b>		<b>A2</b>	
		$\lambda_{\text{abs}}$ (nm), $\epsilon$ ( $\text{L mol}^{-1} \text{cm}^{-1}$ )	$\lambda_{\text{em}}$ (nm), $\phi$ (%)	$\lambda_{\text{abs}}$ (nm), $\epsilon$ ( $\text{L mol}^{-1} \text{cm}^{-1}$ )	$\lambda_{\text{em}}$ (nm), $\phi$ (%)
1	PhMe	429, 43 300	461, 68	443, 78 700	484, 91
2	TBME	421, 45 700	467, 25	437, 76 000	492, 90
3	THF	425, 34 200	470, 12	440, 64 800	510, 29
4	EA	422, 44 800	470, 40	441, 92 600	522, 74
5	$\text{CHCl}_3$	436, 43 800	480, 53	449, 87 100	531, 85
6	DMF	430, 37 300	492, 22	456, 72 400	567, 05
7	MeCN	426, 38 600	492, 13	457, 90 300	572, 08
8 <sup>b</sup>	—	—	608, 11	—	571, 24

<sup>a</sup> Quantum yields ( $\phi$ ) were determined using Prodan as a reference standard (see eqn (1)). <sup>b</sup> Solid-state.



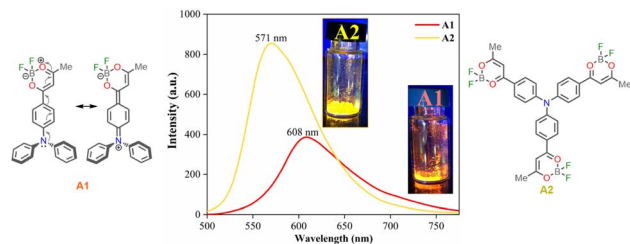


Fig. 2 Fluorescence spectra for dyes **A1** and **A2** in the solid-state at 20 °C,  $\lambda_{\text{ex}} = 350$  nm.

in the solid phase for the dipolar dye **A1**. Another explanation could rely on the formation of J-aggregates that usually show different optical properties from dyes in solution, including red-shifted absorption and emission spectra and enhanced fluorescence quantum yields.<sup>38</sup>

**Response to anions sensing in solution.** Recently, Tamilarasan *et al.*<sup>19</sup> studied compound **A1** as a probe for cyanide sensing applications due to the presence of the dioxaborinine unit as an excellent cyanide-acceptor group. Inspired by these previous studies and our interest in developing molecular probes to detect cyanide,<sup>21,22,31</sup> we envisioned dye **A2** could show an interesting behavior in this sensing field. Thus, the anion sensing property of **A2** was evaluated by treating the probe with  $\text{CN}^-$  and other anions of the potassium or sodium salts (100  $\mu\text{M}$ ), including  $\text{F}^-$ ,  $\text{Cl}^-$ ,  $\text{Br}^-$ ,  $\text{I}^-$ ,  $\text{AcO}^-$ ,  $\text{IO}_4^-$ ,  $\text{PO}_4^{3-}$ ,  $\text{HSO}_4^-$ ,  $\text{HCO}_3^-$ , and  $\text{ClO}^-$  using MeCN/Tris (9 : 1, 1.0 mM at pH 7.5) as a solvent. When  $\text{CN}^-$  (1.4 equiv.) was added to the dye solution, the emission band around 572 nm disappeared, and the color of the solution changed from orange to pale yellow; in contrast, by adding other different anions, except by fluorine ( $\text{F}^-$ ), no substantial changes in the emission spectra were observed (Fig. 3a).

Due to the good preliminary results using the hybrid compound **A2** for anions recognition, titration of **A2** with  $\text{F}^-$  in acetonitrile/Tris was carried out the interaction was monitored by fluorescence at 572 nm (Fig. 3b). Upon the addition of 6.0 equiv. of  $\text{F}^-$ , the emission band at 572 nm decreased linearly with a concentration (conc.) increased from 0 to 60.0  $\mu\text{M}$ ; the limit of detection (LOD), calculated by the expression  $\text{LOD} = 3 \times \text{SD}/\sigma$ , where  $\sigma$  is the slope of the titration curve, and SD is the standard deviation of ten measurements of the blank, for  $\text{F}^-$  was found to be 0.70  $\mu\text{M}$ . These preliminary results allow us to

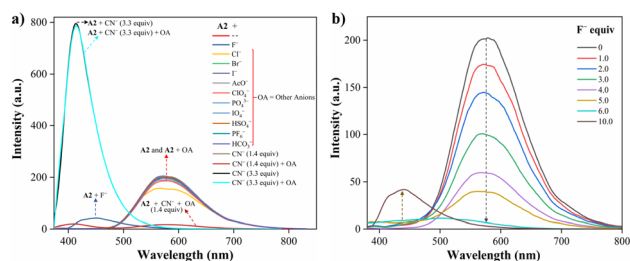


Fig. 3 Emission spectra of **A2** (10.0  $\mu\text{M}$ ,  $\lambda_{\text{ex}} = 350$  nm) in MeCN/Tris (9 : 1) at 20 °C (a) with various anions (100.0  $\mu\text{M}$ ) and  $\text{CN}^-$  (14.0 and 33.0  $\mu\text{M}$ ), and (b) with  $\text{F}^-$  (0–100.0  $\mu\text{M}$ ).

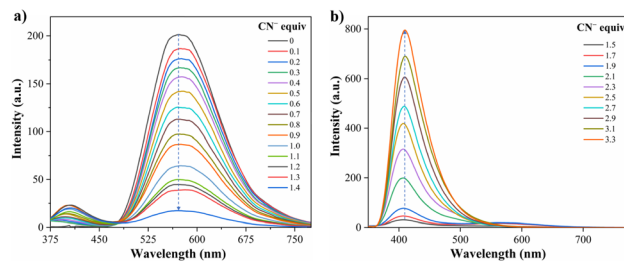


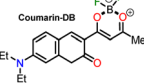
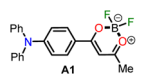
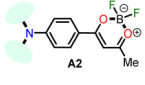


Fig. 4 Emission spectra of **A2** (10.0  $\mu\text{M}$ ,  $\lambda_{\text{ex}} = 350$  nm) in MeCN/Tris (9 : 1) at 20 °C in the presence of  $\text{CN}^-$  (a) 0–14.0  $\mu\text{M}$  and (b) 15.0–33.0  $\mu\text{M}$ .

conclude that the sensitivity of **A2** toward  $\text{CN}^-$  is much higher than that found for  $\text{F}^-$ ; indeed, high fluorine concentrations are needed to complete the decrease in the emission band. Thus, titration with  $\text{CN}^-$  was also carried out to establish dye **A2** as an efficient probe to detect cyanide (Fig. 4). The fluorescence intensity of the emission band at 572 nm in **A2** decreased linearly when the  $\text{CN}^-$  concentration in the range of 0 to 14.0  $\mu\text{M}$  (Fig. 4a). Noticeable, after 1.4 equiv. of  $\text{CN}^-$ , a new emission band appears around 410 nm, and the fluorescence intensity of the band increased linearly with the concentration of  $\text{CN}^-$  in the range of 15.0 to 33.0  $\mu\text{M}$  (Fig. 4b). Finally, the LOD for  $\text{CN}^-$  was evaluated to be 0.18  $\mu\text{M}$  from Fig. S3 and S6.† These results indicate that **A2** is a sensitive probe for  $\text{CN}^-$  sensing by fluorimetric methods, showing a LOD far below the WHO suggestion (1.9  $\mu\text{M}$ ) for drinking water.<sup>39</sup> Moreover, comparing these results with those reported for **A1** ( $\text{LOD} = 0.36 \mu\text{M}$ )<sup>19</sup> indicates that an octupolar architecture improves the cyanide sensing performance.

Several chemosensors containing dioxaborinine core as the signaling subunit have been described recently; therefore,

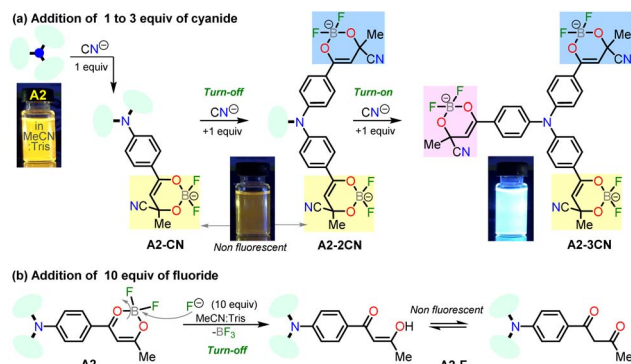
Table 2 Comparison of representative cyanide chemosensors, based on dioxaborinine core, with the new probe **A2**<sup>a</sup>

Compound	Features, LOD, and solvent	Reference
 DMAPh-DB Ar = 4-Me <sub>2</sub> NC <sub>6</sub> H <sub>4</sub>	“Turn on” 2.23 $\mu\text{M}$ , H <sub>2</sub> O $\lambda_{\text{em}} = 620$ nm	Gao <i>et al.</i> <sup>40</sup>
 Ar <sub>2</sub> -DB Ar = 3,4-(OMe) <sub>2</sub> C <sub>6</sub> H <sub>3</sub>	“Turn on” 0.14 $\mu\text{M}$ , H <sub>2</sub> O/MeCN (1 : 4) $\lambda_{\text{abs}} = 649$ nm	Chaicham <i>et al.</i> <sup>41</sup>
 Coumarin-DB Et	“Turn off” 72 nM, PBS/DMSO (3 : 2, pH 7.4) $\lambda_{\text{em}} = 565$ nm	Li <i>et al.</i> <sup>42</sup>
 <b>A1</b>	“Turn on” 0.36 $\mu\text{M}$ , MeCN/H <sub>2</sub> O (98 : 2) $\lambda_{\text{em}} = 402$ nm	Tamilarasan <i>et al.</i> <sup>19</sup>
 <b>A2</b>	“Turn on-off-on” 0.18 $\mu\text{M}$ , MeCN/Tris (9 : 1, pH 7.5) $\lambda_{\text{em}} = 572$ nm	This work

<sup>a</sup> Data were recorded at different concentrations of **A1** and **A2** in THF at 20 °C (see eqn (3)).







Scheme 3 Plausible mechanisms for anions sensing upon addition of (a) 1 to 3 equiv. of  $\text{CN}^-$  or (b) 10 equiv. of  $\text{F}^-$  to solutions of **A2**.

a representative summary of this type of probe compared to the synthesized dye in this work was carried out (Table 2).<sup>19,40–42</sup>

Notably, the new hybrid dye **A2** reported here demonstrates good sensitivity and selectivity with a relatively simple chemical structure and synthetic pathway. Likewise, and due to its trimeric molecular architecture, **A2** is one of the few probes that can detect cyanide ions sequentially through a “turn on-off-on” process (*i.e.*, detection by adding 1 equiv. and then completing up to 3 equiv.). Ultimately, the synthesis of **A2** is carried out by an operationally simple and efficient process compared to other probes synthesized for cyanide recognition (Schemes 2 and 3).

**Proposed mechanism for anions recognition.** The cyanide sensing mechanism for the dipolar dioxaborinine receptor **A1** has already been described as a nucleophilic addition of  $\text{CN}^-$  to the sterically less hindered electrophilic carbon (Scheme 1a).<sup>19</sup> Upon adding 1 or 2 equiv. of  $\text{CN}^-$  ions to the solution of **A2**, the probe emission band at  $\sim 570$  nm disappears with a turn-off fluorescence due to the symmetry broken into the formed complexes **A2-1CN** and **A2-2CN**. However, by adding 3.3 equiv. of  $\text{CN}^-$ , the donor-acceptor architecture in **A2** disappears, and the symmetry is restored; thus, the emission properties now rely on the less  $\pi$ -conjugated tris-vinyl-TPAm moiety in **A2-3CN** ( $\lambda_{\text{em}} = 410$  nm, Fig. S16†), favoring a redshifted turn-on fluorescence concerning **A2** (Scheme 3a). On the other hand, as reported by Yan *et al.*,<sup>43</sup> the  $\text{F}^-$  addition is presumed to proceed with the opening of the dioxaborinine ring in **A2** due to the attack on the boron atom in the probe molecule (Scheme 3b). The mechanistic assumptions cited were tracked by mass spectrometry analysis for adducts **A2-1CN**, **A2-2CN**, and **A2-F** (Fig. S10 and S11†).

**Test strips.** Based on the distinct emission color change of **A2** under a 365 nm hand-held UV lamp in an acetonitrile

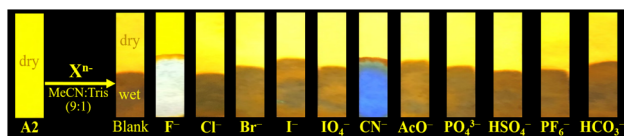


Fig. 5 Images of **A2** test strips prepared on filter paper for the selective detection of  $\text{CN}^-$  and  $\text{F}^-$  in MeCN/Tris (9 : 1) using a hand-held UV lamp ( $\lambda_{\text{ex}} = 365$  nm).

solution by adding cyanide, filter paper immersed with **A2** was proposed to detect this anion. The test strip was prepared by simple immersion of qualitative filter paper (Filter Disc, Ref. 3.303.125, Boeco) in a solution of **A2** in THF (10 mL at 1.2 mM) followed by air-drying under atmospheric conditions (Fig. 5). Subsequent, anions spiked acetonitrile sample (0.1 mM) was dropped onto the strips for naked eye detection under illumination with a hand-held UV lamp without the paper being completely dry. As depicted, the paper containing **A2** displayed bright blue emission only under exposure to cyanide solution. However, the color changed to white after the test strips stained with **A2** were immersed into the acetonitrile solutions with fluoride  $\text{F}^-$  (100.0  $\mu\text{M}$ ). Based on the distinctive color change of **A2** when exposed to  $\text{CN}^-$  this compound proved that the test strips could be applied to detect  $\text{CN}^-$  and  $\text{F}^-$  anions qualitatively in a rapid way.

**Preliminary two-photon absorption properties.** The preliminary TPA properties of **A1** and **A2** in THF were studied by detecting two-photon-induced emissions. The detected fluorescence is shown as a function of the laser light power for different concentrations of dyes (Fig. 6). The dots correspond to experimental measurements, and the dashed lines are quadratic fits to the data ( $R^2/\text{conc. in mM}$ : **A1** = 0.999/1.0, 0.996/5.0, and 0.999/10.0; **A2** = 0.968/1.0, 0.9982/0.1, 0.999/1.0, and 0.997/5.0). From the fitting parameters, the experimental value for the two-photon excitation action cross-section ( $\sigma'$ ) can be obtained according to eqn (3) (see the Experimental section). The values obtained for  $\sigma'$  for diverse concentrations of **A1** and **A2** are also reported (Table 3). The technique was verified by measuring the  $\sigma'$  using rhodamine B (RB) in methanol to

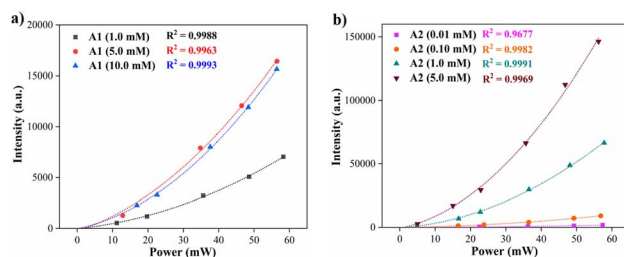


Fig. 6 Two-photon induce fluorescence signal as a function of the laser power of compounds (a) **A1** and (b) **A2** at different concentrations in THF (20 °C).

Table 3 Two-photon excitation action cross section for dyes **A1** and **A2**<sup>a</sup>

Concentration (mM)	$\sigma'$ (GM)	
	<b>A1</b>	<b>A2</b>
0.01	—	20 ± 4
0.10	—	12 ± 2
1.00	0.49 ± 0.09	8.8 ± 1.6
5.00	0.25 ± 0.05	4.3 ± 0.8
10.00	0.12 ± 0.02	—

<sup>a</sup> Data were recorded at different concentrations of **A1** and **A2** in THF at 20 °C (see eqn (3)).

0.05 mM.<sup>44</sup> The value obtained in the experiment is  $\sigma' = 4.4 \pm 0.7$  GM. Considering the value of  $\phi$  reported in the literature for RB,<sup>45</sup> herein we report a TPA cross-section  $\delta = 6.8 \pm 1.8$  GM that agrees with the previously reported values (Table S2†). Notably, values found for **A2** are in the same order of magnitude as RB under similar conditions.

The results of two-photon absorption experiments demonstrate that the hybrid fluorophores **A1** and **A2** can induce such processes. The values obtained for the two-photon excitation action cross-section show that trimeric compound **A2** has a higher probability of a two-photon induced fluorescence process when compared with the analog monomeric **A1**. This effect can be attributed to the geometry differences between **A1** (dipolar) and **A2** (octupolar) since the TPA cross-section in octupoles could scale three times the corresponding values in the isolated dipolar analogs.<sup>17,46–48</sup> Values of the cross sections in Table 3 change due to variation in the fluorescence quantum yield with the concentration<sup>46</sup> and the possibility of aggregation effects at higher concentrations. Finally, the respective representative diagrams of the z-scan system and the fluorescence process were made (Fig. S18†) to clarify the optical route by which the fluorescence induced by two-photon occurs. Specifically, Jablonski diagrams in Fig. S18b† show the difference between linear fluorescence and two-photon excitation, clarifying the two-photon absorption mechanism of the fluorophore **A2**.

## Conclusions

In summary, a highly fluorescent trimeric probe **A2** was synthesized using a one-pot methodology, and its photophysical properties were examined. This compound displays high fluorescence quantum yields in solvents with low to medium polarity ( $\phi$  of 0.91 MePh to 0.85 CHCl<sub>3</sub>), interesting emission quantum yield at solid-state ( $\phi = 0.24$  to 571 nm), and moderate solvatochromism from toluene (485 nm) to acetonitrile (572 nm). The nucleophilic addition reaction of CN<sup>−</sup> or F<sup>−</sup> on the dioxaborinine ring changes the emission properties of the **A2** solution, giving selective fluorometric detection of these anions with limits of detection of 0.18 and 0.70  $\mu$ M, respectively. In addition, a test strip assay using **A2** has also been applied to detect CN<sup>−</sup> or F<sup>−</sup> in organic solutions. Noticeably, CN<sup>−</sup> can be discriminated from F<sup>−</sup> by tracking the emission at 410 nm. Ultimately, a clear two-photon induce process was observed for **A1** and **A2**. In particular, the two-photon excitation action cross section of **A2** shows that this probe can be exploited, as rhodamine B, in different applications, e.g., two-photon microscopy or non-linear optics for the ion sensing field. The extension of the  $\pi$ -conjugation and the possibility of a symmetry-broken dipolar state induce better photophysical properties in compound **A2** than its dipolar analog **A1**.

## Experimental section

### Reagents and materials

**Synthesis.** Reagents were purchased from commercial sources and used without further purification; these were weighed

and handled in the air at room temperature. The reaction was monitored by thin-layer chromatography (TLC), visualized by a UV lamp (254 or 365 nm), and flash chromatography was performed on silica gel (230–400 mesh). The methyl ketone precursor (4-acetylphenyl)diphenylamine (**2**) was obtained in a 67% yield using a known method starting from triphenylamine (**1**).<sup>33</sup> Subsequently, the  $\beta$ -diketone intermediate 1-(4-(diphenylamino)phenyl)butane-1,3-dione (**3**) was prepared in a 78% yield from methyl ketone **1** (Scheme 2a).<sup>19</sup>

**Characterization.** For the structural characterization of the hybrid compounds **A1** and **A2**, their NMR spectra (Fig. S1–S7†) were recorded at 400 MHz (<sup>1</sup>H), 101 MHz (<sup>13</sup>C{<sup>1</sup>H}), and 374 MHz (<sup>19</sup>F) at 25 °C using CDCl<sub>3</sub> or DMSO-*d*<sub>6</sub> as solvents and tetramethylsilane (TMS,  $\delta$ : 0 ppm) as the internal reference. The chemical shifts ( $\delta$ ) are reported in ppm, and the coupling constants (*J*) are reported in Hz. The following abbreviations are used for multiplicities: s = singlet, d = doublet, and m = multiplet. The melting point was collected using a capillary melting point apparatus and is uncorrected. The high-resolution mass spectra (HRMS) for the hybrid dyes **A1** and **A2** (Fig. S8 and S9†) were obtained on an Agilent Technologies Q-TOF 6520 spectrometer *via* electrospray ionization (ESI). The mass spectra for adducts **A2-1CN**, **A2-2CN**, and **A2-F** (Fig. S10 and S11†) were recorded on a Thermo-Scientific LCQ Fleet™ ion-trap mass spectrometer using positive ion mode ESI and a direct inlet system.

Regarding the photophysical studies of **A1** and **A2**, absorption (UV-vis) and emission spectra were recorded at room temperature (20 °C) in an air-equilibrated solution on Varian Cary 100 and Cary Eclipse spectrophotometers, respectively (both are Agilent Technologies devices) using quartz cuvettes with a path length of 1 cm. For fluorescence studies, both the excitation and emission slit widths were 5 nm. The fluorescence quantum yields ( $\phi$ ) were determined using Prodan<sup>49</sup> as a reference standard by eqn (1)

$$\phi_{f,x} = \phi_{f,st} \frac{F_x}{F_{st}} \frac{A_{st}}{A_x} \frac{n_x^2}{n_{st}^2} \quad (1)$$

where *F* is the integral photon flux, *A* is the absorption factor, *n* is the solvent refractive index,  $\phi_f$  is the quantum yield. The indexes *x* and *st* denote the sample and standard, respectively.<sup>50</sup>

On the other hand, Catalán's multiparametric relationship can be formulated by eqn (2)

$$A = A_0 + bSA + cSB + dSP + eSdP \quad (2)$$

where *A* is a solvent-dependent physicochemical property in a given solvent, and *A*<sub>0</sub> is the statistical quantity agreeing to the value of the property in the gas phase; SA, SB, SP, and SdP represent independent yet complementary solvent parameters accounting for various types of solute–solvent interactions; and *b* to *e* are the regression coefficients relating the sensitivity of property *A* to the different solute–solvent interaction mechanisms.<sup>51</sup>

Finally, the two-photon excitation action cross section ( $\sigma'$ ) was measured using a continuous-wave (CW) laser at 817 nm



when driving the two-photon transition. The laser light was focused on the sample contained in a 1 mm thick quartz cuvette, employing an objective microscope lens. The sample was placed on a translational stage that allows for implementing the z-scan technique. The fluorescence was detected as a function of the position of the sample by a photomultiplier tube. The dependence of the fluorescence signal ( $F$ ) with the power of the laser light ( $P$ ) is given by eqn (3)

$$F \approx g\eta\sigma' C \frac{4nP^2}{\pi\lambda} \quad (3)$$

where  $g$  is the temporal second-order correlation function of the incoming light source,  $\eta$  is overall fluorescence collection efficiency,  $n$  is the refractive index of the solvent,  $C$  is the sample concentration, and  $\sigma' = \phi\delta$  ( $\phi$  is the quantum yield and  $\delta$  the TPA cross-section).<sup>45</sup>

### Synthesis and characterization

**4-(2,2-Difluoro-6-methyl-2H-1 $\lambda^3$ ,3,2 $\lambda^4$ -dioxaborinin-4-yl)-N,N-diphenylaniline (A1).** To a stirred solution of the freshly synthesized (54% for the two steps from **1**)  $\beta$ -diketone **3** (0.12 g, 0.36 mmol) in dichloromethane (DCM, 5.0 mL),  $\text{BF}_3 \cdot \text{OEt}_2$  (0.054 mL, 0.44 mmol) was added dropwise at room temperature and maintained for 30 min. The reaction mixture color changed instantly to red during the  $\text{BF}_3 \cdot \text{OEt}_2$  addition. The reaction was quenched with aqueous NaOH solution 0.5 M and extracted with  $\text{DCM} \times 3$ . The crude product was purified by column chromatography in silica gel (DCM as eluent) to obtain **A1** as a red solid in a 96% yield. Mp: 209–212 °C.  $^1\text{H}$  NMR (401 MHz,  $\text{CDCl}_3$ ):  $\delta$  = 2.33 (s, 3H), 6.37 (s, 1H), 6.94 (d,  $J$  = 8.9 Hz, 2H), 7.26–7.17 (m, 6H), 7.38 (t,  $J$  = 7.7 Hz, 4H), 7.94–7.80 (m, 2H) ppm.  $^{13}\text{C}$  NMR (100 MHz,  $\text{CDCl}_3$ ):  $\delta$  = 24.4, 95.9, 118.3, 121.5, 126.0, 126.7, 130.0, 131.3, 145.3, 154.5, 180.9, 188.2 ppm.  $^{19}\text{F}$  NMR (374 MHz,  $\text{CDCl}_3$ ):  $\delta$  = –139.9 ppm. HRMS (ESI)  $m/z$ :  $[\text{M} - \text{F}]^+$  calcd for  $\text{C}_{22}\text{H}_{18}\text{BFNO}_2^+$  358.1415; found 358.1409. These data matched those previously reported.<sup>19</sup>

**Tris(4-(2,2-difluoro-6-methyl-2H-1 $\lambda^3$ ,3,2 $\lambda^4$ -dioxaborinin-4-yl)phenyl)amine (A2).** To a stirred solution of triphenylamine (1, 0.245 g, 1.0 mmol) in acetic anhydride (1.0 mL),  $\text{BF}_3 \cdot \text{OEt}_2$  (0.5 mL) was added dropwise at 60 °C and maintained for 5 h. The reaction mixture color changed instantly to black during the addition of  $\text{BF}_3 \cdot \text{OEt}_2$ . The reaction was quenched with aqueous  $\text{NH}_3$  solution 0.5 M and extracted with  $\text{DCM} \times 3$ . The crude product was purified by column chromatography in silica gel (DCM as eluent) to obtain **A2** as an orange solid in a 52% yield. Mp: 210–211 °C.  $^1\text{H}$  NMR (400 MHz,  $\text{DMSO}-d_6$ )  $\delta$ : 2.45 (s, 9H), 7.23 (s, 3H), 7.36 (d,  $J$  = 8.5 Hz, 6H), 8.20 (d,  $J$  = 8.5 Hz, 6H) ppm.  $^{13}\text{C}$  NMR (101 MHz,  $\text{DMSO}-d_6$ )  $\delta$ : 24.4 ( $\text{CH}_3$ ), 97.9 (CH), 124.9 (CH), 126.4 (C), 131.3 (CH), 151.4 (C), 179.7 (C), 193.2 (C=O) ppm.  $^{19}\text{F}$  NMR (374 MHz,  $\text{CDCl}_3$ ):  $\delta$  = –137.8 ppm. HRMS (ESI)  $m/z$ :  $[\text{M} - \text{F}]^+$  calcd for  $\text{C}_{30}\text{H}_{24}\text{B}_3\text{F}_5\text{NO}_6^+$  622.1798; found 622.1816.

### Conflicts of interest

The authors declare no competing financial interest.

### Acknowledgements

We wish to thank the Departments of Chemistry and Physics and Vicerrectoría de Investigaciones at the Universidad de Los Andes for financial support. M. N.-P. and J. P. acknowledge support from the science faculty (projects INV-2020-105-2083 and INV-2019-84-1800). We also acknowledge Sandra Ortiz of Universidad de Los Andes for acquiring the mass spectra.

### Notes and references

- 1 D. Cappello, R. R. Maar, V. N. Staroverov and J. B. Gilroy, *Chem.-Eur. J.*, 2020, **26**, 5522–5529.
- 2 J.-L. Jin, L. Yang, X. Ding, L.-H. Ou, Y.-D. Chen, H.-Y. Gu, Y. Wu and Y. Geng, *ACS Omega*, 2020, **5**, 21067–21075.
- 3 A. Filarowski, M. Lopatkova, P. Lipkowski, M. van der Auweraer, V. Leen and W. Dehaen, *J. Phys. Chem. B*, 2015, **119**, 2576–2584.
- 4 M. Más-Montoya, M. F. Montenegro, A. E. Ferao, A. Tárraga, J. N. Rodríguez-López and D. Curiel, *Org. Lett.*, 2020, **22**, 3356–3360.
- 5 V. Ramu, S. Gautam, P. Kondaiah and A. R. Chakravarty, *Inorg. Chem.*, 2019, **58**, 9067–9075.
- 6 X. Ren, F. Zhang, H. Luo, L. Liao, X. Song and W. Chen, *Chem. Commun.*, 2020, **56**, 2159–2162.
- 7 W.-J. Shi, Y.-F. Wei, C.-F. Li, H. Sun, L.-X. Feng, S. Pang, F. Liu, L. Zheng and J. Yan, *Spectrochim. Acta, Part A*, 2021, **248**, 119207.
- 8 H. Zhang, J. Xing, J. Peng, J. Bai, J. Zhang, D. Fu and J. Jia, *J. Lumin.*, 2022, **241**, 118525.
- 9 M. Pawlicki, H. A. Collins, R. G. Denning and H. L. Anderson, *Angew. Chem., Int. Ed.*, 2009, **48**, 3244–3266.
- 10 R. Medishetty, J. K. Zaręba, D. Mayer, M. Samoć and R. A. Fischer, *Chem. Soc. Rev.*, 2017, **46**, 4976–5004.
- 11 Q. Geng, C. Gu, J. Cheng and S. Chen, *Optica*, 2017, **4**, 674.
- 12 F. Bolze, S. Jenni, A. Sour and V. Heitz, *Chem. Commun.*, 2017, **53**, 12857–12877.
- 13 V. Juvekar, C. S. Lim, D. J. Lee, S. J. Park, G. O. Song, H. Kang and H. M. Kim, *Chem. Sci.*, 2021, **12**, 427–434.
- 14 Q. Geng, D. Wang, P. Chen and S.-C. Chen, *Nat. Commun.*, 2019, **10**, 2179.
- 15 X. Lou, Z. Zhao and B. Z. Tang, *Small*, 2016, **12**, 6430–6450.
- 16 S. Pascal, S. David, C. Andraud and O. Maury, *Chem. Soc. Rev.*, 2021, **50**, 6613–6658.
- 17 D. Beljonne, W. Wenseleers, E. Zojer, Z. Shuai, H. Vogel, S. J. K. Pond, J. W. Perry, S. R. Marder and J.-L. Brédas, *Adv. Funct. Mater.*, 2002, **12**, 631–641.
- 18 M. Collot, *Mater. Horiz.*, 2021, **8**, 501–514.
- 19 D. Tamilarasan, R. Suhasini, V. Thiagarajan and R. Balamurugan, *Eur. J. Org. Chem.*, 2020, **2020**, 993–1000.
- 20 S.-L. Aranzazu, A. Tigreros, A. Arias-Gómez, J. Zapata-Rivera and J. Portilla, *J. Org. Chem.*, 2022, **87**, 9839–9850.
- 21 A. Tigreros and J. Portilla, *Eur. J. Org. Chem.*, 2022, **2022**, e202200249.
- 22 M.-C. Ríos, N.-F. Bravo, C.-C. Sánchez and J. Portilla, *RSC Adv.*, 2021, **11**, 34206–34234.



- 23 G. Delhumeau, A. M. Cruzmendoza and C. G. Lojero, *Toxicol. Appl. Pharmacol.*, 1994, **126**, 345–351.
- 24 H. Kaur and P. Singh, *Bioorg. Chem.*, 2019, **82**, 229–240.
- 25 R. Kaushik, A. Ghosh, A. Singh, P. Gupta, A. Mittal and D. A. Jose, *ACS Sens.*, 2016, **1**, 1265–1271.
- 26 S. Malkondu, S. Erdemir and S. Karakurt, *Dyes Pigm.*, 2020, **174**, 108019.
- 27 P. Xing, Y. Xu, H. Li, S. Liu, A. Lu and S. Sun, *Sci. Rep.*, 2015, **5**, 16528.
- 28 N. Bortey-Sam, R. Jackson, O. A. Gyamfi, S. Bhadra, C. Freeman, S. B. Mahon, M. Brenner, G. A. Rockwood and B. A. Logue, *Anal. Chim. Acta*, 2020, **1098**, 125–132.
- 29 A. Tigreros, M. Macías and J. Portilla, *Dyes Pigm.*, 2021, **184**, 108730.
- 30 A. Tigreros, M. Macías and J. Portilla, *Dyes Pigm.*, 2022, **202**, 110299.
- 31 A. Tigreros, J. Zapata-Rivera and J. Portilla, *ACS Sustainable Chem. Eng.*, 2021, **9**, 12058–12069.
- 32 S.-J. Chung, K.-S. Kim, T.-C. Lin, G. S. He, J. Swiatkiewicz and P. N. Prasad, *J. Phys. Chem. B*, 1999, **103**, 10741–10745.
- 33 Q. Zhang, P. Jiang, K. Wang, G. Song and H. Zhu, *Dyes Pigm.*, 2011, **91**, 89–97.
- 34 L. D. Costa, S. Guieu, J. Rocha, A. M. S. Silva and A. C. Tomé, *New J. Chem.*, 2017, **41**, 2186–2192.
- 35 S. Easwaramoorthi, P. Thamaraiselvi, K. Duraimurugan, A. J. Beneto, A. Siva and B. U. Nair, *Chem. Commun.*, 2014, **50**, 6902–6905.
- 36 L. Wu, J. Liu, P. Li, B. Tang and T. D. James, *Chem. Soc. Rev.*, 2021, **50**, 702–734.
- 37 V. Parthasarathy, S. Fery-Forgues, E. Campioli, G. Recher, F. Terenziani and M. Blanchard-Desce, *Small*, 2011, **7**, 3219–3229.
- 38 K. Li, X. Duan, Z. Jiang, D. Ding, Y. Chen, G.-Q. Zhang and Z. Liu, *Nat. Commun.*, 2021, **12**, 2376.
- 39 X. He, X. Wang, L. Zhang, G. Fang, J. Liu and S. Wang, *Sens. Actuators, B*, 2018, **271**, 289–299.
- 40 Y. Gao, M. Li, X. Tian, K. Xu, S. Gong, Y. Zhang, Y. Yang, Z. Wang and S. Wang, *Spectrochim. Acta, Part A*, 2022, **271**, 120882.
- 41 A. Chaicham, S. Kulchat, G. Tumcharern, T. Tuntulani and B. Tomapatanaget, *Tetrahedron*, 2010, **66**, 6217–6223.
- 42 S. Li, F. Huo, K. Ma, Y. Zhang and C. Yin, *New J. Chem.*, 2021, **45**, 1216–1220.
- 43 N. Yan, F. Wang, J. Wei, J. Song, L. Yan, J. Luo, Z. Fang, Z. Wang, W. Zhang and G. He, *Dyes Pigm.*, 2019, **166**, 410–415.
- 44 C. B. Malagon, M. Pellaton, A. Tigreros, J. Portilla, A. Valencia and M. N. Portela, in *OSA Nonlinear Optics 2021*, Optica Publishing Group, Washington, D.C., 2021, p. NTh3A.13.
- 45 C. Xu and W. W. Webb, *J. Opt. Soc. Am. B*, 1996, **13**, 481.
- 46 C. v. Bindhu, S. S. Harilal, G. K. Varier, R. C. Issac, V. P. N. Nampoori and C. P. G. Vallabhan, *J. Phys. D: Appl. Phys.*, 1996, **29**, 1074–1079.
- 47 M. G. Vivas, D. L. Silva, J. Malinge, M. Boujtita, R. Zaleśny, W. Bartkowiak, H. Ågren, S. Canuto, L. de Boni, E. Ishow and C. R. Mendonca, *Sci. Rep.*, 2015, **4**, 4447.
- 48 C. Katan, F. Terenziani, O. Mongin, M. H. v. Werts, L. Porrès, T. Pons, J. Mertz, S. Tretiak and M. Blanchard-Desce, *J. Phys. Chem. A*, 2005, **109**, 3024–3037.
- 49 Y. Niko, S. Kawauchi and G. Konishi, *Chem.–Eur. J.*, 2013, **19**, 9760–9765.
- 50 C. Würth, M. Grabolle, J. Pauli, M. Spieles and U. Resch-Genger, *Nat. Protoc.*, 2013, **8**, 1535–1550.
- 51 J. Catalán, *J. Phys. Chem. B*, 2009, **113**, 5951–5960.

